ELSEVIER

Chemical Engineering Journal 108 (2005) 219–226

Chemical Engineering Journal

www.elsevier.com/locate/cej

The temperature-scanning plug flow reactor (TSPFR) applied to complex reactions—Oxidative dehydrogenation of propane as an example

Matthias Kolkowski [a], Frerich J. Keil [a,*], Christian Liebner [b], Dorit Wolf [b], Manfred Baerns [b]

[a] *Hamburg University of Technology, Chemical Reaction Engineering, Eissendorfer Str. 38, D-21073 Hamburg, Germany*
[b] *Institute for Applied Chemistry Berlin Adlersdorf, Richard-Willstätter Str. 12, D-12489 Berlin, Germany*

Received 28 April 2004; received in revised form 3 February 2005; accepted 8 February 2005

Abstract

The temperature-scanning plug flow reactor (TSPFR) enables the investigation of kinetics of chemical reactions over a wide temperature range in a relatively small time of operation. The experimental data obtained by this approach can be used to calculate the reaction rate of each component of the reactant mixture for a given set of conditions. The oxidative dehydrogenation of propane by a $V_2O_5/\gamma\text{-}Al_2O_3$ catalyst was used for illustration. As this reaction is highly exothermic some limitations of the approach had to be considered.

Keywords: Temperature-scanning plug flow reactor; Oxidative dehydrogenation of propane

1. Introduction

Reliable kinetic data are of outstanding importance in reactor design and optimization. Inaccurate kinetic data spoil any reactor modelling. Kinetic measurements are very time consuming and involved. Therefore, it is desirable to introduce more efficient approaches in kinetic experimentation. In 1997, Wojciechowski and co-workers published a series of articles about the temperature-scanning reactor (TSR) [1–3], which allows to perform kinetic experiments in fully automated reactors in a far shorter time than in conventional devices. According to some industrial announcements, the TSR could accelerate measurements by a factor of up to ten. A major problem is the data evaluation algorithm, which has not been described in detail in the original paper by Wojciechowski [1]. Liebner et al. [4] developed an algorithm for effective evaluation of kinetic data of the temperature-scanning reactor and executed experimental tests on this reactor by employing the ammonia synthesis reaction. The reactor, combined with an appropriate mode of operation and approach of data evaluation, gave reliable values of reaction rates for non-isothermal reactor operation in an integral range of conversion and a range of conversion including thermodynamic equilibrium, respectively. Thus, a large amount of data can be obtained leading to a well-founded basis of kinetic modelling. Kolkowski et al. [5] discussed sources of error in this type of reactor. The influence of heat transport phenomena on the reaction rate data obtained by the temperature-scanning plug flow reactor (TSPFR) was investigated by means of simulation. The main advantages of the TSPFR can be summed up like this:

- fast kinetic investigations over a large temperature range are possible;
- automation of the entire device is possible;
- a large amount of data can be monitored in a rather short time;
- the TSPFR is simple to implement and requires only standard hardware.

Contrary to the ammonia synthesis, in the present paper a complex irreversible reaction was investigated by the TSPFR, namely the oxidative dehydrogenation of propane. This reaction is extremely exothermic, and should reveal supposable limitations of the TSPFR approach. Resorts from these limitations will be discussed.

* Corresponding author. Tel.: +49 40 42878 3042; fax: +49 40 42878 2145.
E-mail address: keil@tuhh.de (F.J. Keil).

1385-8947/$ – see front matter © 2005 Elsevier B.V. All rights reserved.
doi:10.1016/j.cej.2005.02.017

Nomenclature

Bi	Biot number
c	concentration (mol/m^3)
D_{ax}	axial dispersion coefficient (m^2/s)
d_i	inner tube diameter (m)
d_p	pellet diameter (m)
E_A	activation energy (J/mol)
h	number of a certain measurement point
k	reaction rate constant (mol/(kg Pa s))
k_o	overall heat transfer coefficient (W/(m^{2}K))
K_{O_2}	adsorption constant of oxygen (Pa$^{-1.5}$)
l	equivalent length (m)
L	length of the reactor (m)
m_{cat}	mass of catalyst (kg)
$\dot{n}$	molar flow rate (mol/s)
N_a	reaction number
N_i	number of a certain residence time
N_j	number of a temperature interval
p	pressure (Pa)
r	radius inside the catalyst packing (m)
r^*	collocation point (radius) (m)
r_i	inner tube diameter (m)
r_{Ri}	reaction rate of reaction i (mol/(kg s))
r_{TS}	reaction rate from experiments (mol/(kg s))
s	residence time (s)
t	time (s)
u_{LR}	superficial gas velocity (m/s)
T	temperature (K)
$T^*(r^*)$	temperature at the collocation radius r^* (K)
$\dot{V}$	volumetric flow (m^3/s)
x	molar fraction

Greek letters

$\delta(t)$	see Eq. (2)
λ_{cat}	heat conductivity of catalyst (W/(m K))
ν_{ij}	stoichiometric constant of component i in reaction j

2. Experimental

The experimental set-up is presented in Fig. 1. The experiments were carried out in a quartz tube reactor. The reactor was placed in an oven with rapidly circulating air. The outer surface temperature of the reactor should be the same at any position. The oven temperature was controlled by microprocessor controllers. The flows of the inlet gases were controlled by electronic mass flow meters (Bronkhorst F 201 C). Gases of better than 99.9% purity were used. For gas analysis, a micro-gas chromatograph (Varian Chrompack CP 2002) was applied. The sampling by the GC inlet system was done at the exit of the catalyst bed, i.e., inside the reactor tube. A carefully heated capillary and GC inlet system was used to avoid condensing of reaction products. As catalyst V_2O_5/γ-Al_2O_3 was chosen as it provides high propene yields at moderate temperatures. Furthermore, this catalyst is robust and can be regenerated. The catalyst was manufactured in the following way: 0.822 g V_2O_5 and 0.5 g polyvinyl acetate were slowly added to a stirred solution of 2 g oxalic acid in 130 ml H_2O at 75 °C. The clear liquid is cooled down to room temperature and mixed with 5 g γ-AlO(OH). After having stirred this solution for 15 min, γ-Al_2O_3 was slowly added. The catalyst was dried for 24 h at 60 °C, and then calcinated for 6 h at 600 °C in stagnant air. The catalyst has initially a green-yellow colour and turns to green, like chromium oxide, after usage. Its BET surface was 130 m^2/g. XRD analysis showed only γ- and δ-Al_2O_3 phases. The catalyst (V_2O_5/γ-Al_2O_3 diluted with SiO_2 particles (1:5) because of the high exothermicity of the reaction) has to be evenly distributed along the reactor in order to have a uniform effectiveness along the reactor. A feed of constant gas composition and flow is supplied to the reactor inlet. The inlet gas is heated according to a defined temperature program before entering the reactor. The reactants preheating unit is installed inside the oven. The temperature is recorded at the inlet and the outlet of the reactor. The gas composition is also measured at the outlet. After having run the temperature program, the reactor is cooled down to the temperature level of the previous run. During the cooling down period, the catalyst was regenerated by pure oxygen flowing through the catalyst bed. This resulted in a reproducible activity for each of the operated temperature ramps. Then, a different flow rate of the reactants is adjusted, and exactly the same temperature ramp is operated. The temperature of the surrounding air with which the reactor exchanges heat must be ramped in the same way, from the same starting temperature, in each run. This ensures that the driving forces for heat fluxes between the reactor and its surroundings are the same from run to run. This procedure is repeated for a defined number of different reactant volume flow rates, which correspond to different residence times inside the reactor. The TSPFR gives, without approximation or extrapolation, conventional multiplets of conversion/yields–rates–temperatures. After certain time intervals, data like experiment run time, t_i, oven temperature, T_{oven}, reactor inlet temperature, T_{in}, reactor outlet temperature, T_{out}, and the mole fractions, x_i, of all species in the outlet gas are measured. To make such data interpretable, the temperature ramping rate has to be such that the time between successive analyses is much shorter than the time required for a kinetically significant increment of temperature to be induced in the feed to the reactor. The pressure and the composition of the reactants have to be the same in all runs. Inside the reactor, plug flow conditions have to exist. As a consequence, there should be nearly no radial temperature profile in the catalyst bed. Hot spots have to be avoided. These conditions have to be checked. As the details of the TSPFR theory are given by Liebner et al. [4], only a few remarks about the data evaluation of the TSPFR will be given here. The foundation of the evaluation of kinetic data by means

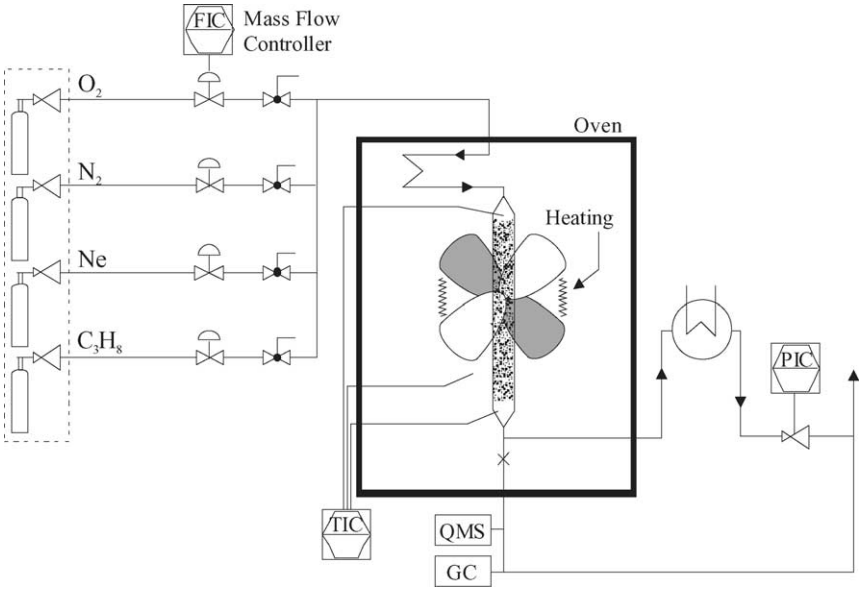

Fig. 1. Experimental set-up of the temperature-scanning plug flow reactor (TSPFR).

of the TSPFR approach starts with te material balance of an ideal stationary tubular reactor:

$$0 = -\frac{\mathrm{d}(c_i \dot{V})}{\mathrm{d}m_{\mathrm{cat}}} + \sum v_{ij} r_j \,(\mathrm{mol/(kg\,s)}) \tag{1}$$

To transfer this equation to a tubular reactor of constant length, whereby the residence time is varied for a constant catalyst mass, a factor $\delta(t)$ is defined, which is the ratio of the volume flow rate at the exit of the reactor at time t, $\dot{V}_{\mathrm{out}}(t)$, to the volume flow rate at the reactor inlet at that time, $\dot{V}_{\mathrm{in}}(t-s)$. The catalyst contact time, s, is the actual residence time of a volume element of the fluid in the catalyst packing. That means $\delta(t)$ is a measure for the relative volume change of a volume element owing to temperature change and chemical reaction.

$$\delta(t) = \frac{\dot{V}_{\mathrm{out}}(t)}{\dot{V}_{\mathrm{in}}(t-s)} \tag{2}$$

Inserting Eq. (2) into Eq. (1) gives:

$$0 = -\dot{V}_{\mathrm{in}}(t-s)\left.\frac{\mathrm{d}(c_i \delta(t))}{\mathrm{d}m_{\mathrm{cat}}}\right|_{T_{\mathrm{in}}} + \sum v_{ij} r_j \,(\mathrm{mol/(kg\,s)}) \tag{3}$$

Note that $\dot{V}_{\mathrm{in}}(t-s)$ is constant for a constant reactor inlet temperature. In order to determine $\delta(t)$, the volume flow rates at the reactor inlet and outlet have to be measured. In the actual experiment, the volume flow rates, $\dot{V}_{\mathrm{ref}}$, are measured under ambient conditions, which are the reference (P_{ref} = 1 bar, T_{ref} = 298 K). By means of the perfect gas law (or an equation of state, if necessary), this flow rate can be converted into the inlet and outlet conditions of the reactor, as the temperatures, pressures and compositions of the gases are known. In order to include the volume change owing to chemical reaction, an inert component is added to the reactants. The ratio of the mole fraction at the reactor inlet to the mole fraction at the outlet gives the change of the volume flow rate owing to reactions. The outlet volume flow rate is multiplied with this ratio:

$$\dot{V}_{\mathrm{out}}(t) = \dot{V}_{\mathrm{ref}} \frac{P_{\mathrm{ref}}}{P_{\mathrm{out}}(t)} \frac{T_{\mathrm{out}}(t)}{T_{\mathrm{ref}}} \frac{x_{\mathrm{in,inert}}}{x_{\mathrm{out,inert}}}$$
$$= \dot{V}_{\mathrm{ref}} \frac{P_{\mathrm{ref}}}{P_{\mathrm{out}}(t)} \frac{T_{\mathrm{out}}(t)}{T_{\mathrm{ref}}} \frac{\dot{n}_{\mathrm{out}}(t)}{\dot{n}_{\mathrm{in}}(t)} \,(\mathrm{m^3/s}) \tag{4}$$

$$\dot{V}_{\mathrm{in}}(t-s) = \dot{V}_{\mathrm{ref}} \frac{P_{\mathrm{ref}}}{P_{\mathrm{in}}} \frac{T_{\mathrm{in}}(t-s)}{T_{\mathrm{ref}}} \,(\mathrm{m^3/s}) \tag{5}$$

Eqs. (4) and (5) are inserted into Eq. (2):

$$\delta(t) = \frac{P_{\mathrm{ref}}}{P_{\mathrm{out}}(t)} \frac{T_{\mathrm{out}}(t)}{T_{\mathrm{in}}(t-s)} \frac{x_{\mathrm{in,inert}}}{x_{\mathrm{out,inert}}(t)} \tag{6}$$

By means of Eqs. (5) and (6) one can simplify Eq. (3). Additionally a residence time, which is related to the catalyst mass, is introduced:

$$\mathrm{d}\tau_{\mathrm{cat}} = \frac{\mathrm{d}m_{\mathrm{cat}}}{\dot{V}_{\mathrm{ref}}} \,(\mathrm{kg\,s/m^3}) \tag{7}$$

Finally, one obtains an equation for the data evaluation of TSPFR experiment:

$$\frac{\dot{n}_{\mathrm{ref}}}{\dot{V}_{\mathrm{ref}}} x_{\mathrm{in,inert}} \frac{\mathrm{d}}{\mathrm{d}\tau_{\mathrm{cat}}} \left(\frac{x_i(t, \tau_{\mathrm{cat}})}{x_{\mathrm{out,inert}}(t, \tau_{\mathrm{cat}})} \right) \Bigg|_{T_{\mathrm{in}}}$$
$$= \sum \nu_{ij} r_j \,(\mathrm{mol/(kg\,s)}) \tag{8}$$

All the data required in Eq. (8) are obtained from the TSPFR experiment. The experimental conditions employed in the present investigations are given in Table 1. The details of data evaluation are given by Liebner et al. [4].

Table 1
Experimental conditions

Reactor data	
Wall material	Quartz
Length, L_0 (mm)	20
Outer diameter, d_o (mm)	8
Inner diameter, d_i (mm)	6
Heat conductivity quartz, λ_W (W/(m K))	1.2
Catalyst bed	
Catalyst (diluted with SiO_2 (1:5))	V_2O_5/γ-Al_2O_3
Particle diameter, d_p (mm)	0.25–0.35
Sample weight, m_{cat} (g)	0.25
Porosity, ε	0.4
Reaction conditions	
Inlet pressure (Pa)	1.013×10^5
Temperature range (K)	600–750
Temperature program, T_{in} (K)	$\beta \times t + T_{in,start}$
Rate of temperature increase, β (K/min)	2
Run time, t (min)	75

In the present experiments, the oxidative dehydrogenation of propane to propene was investigated:

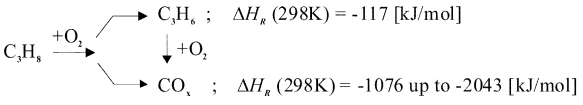

(9)

As the reactions are highly exothermic, it has to be checked whether the heating program changes the catalytic activity. The references were experiments under isothermal and stationary conditions. Measurements were done for heating rates of 1, 2, 5 and 10 K/min. The heating rates employed had no significant influence on the concentrations. As an example, this is demonstrated for propene in Fig. 2. A heating rate of 2 K/min in the subsequent experiments is therefore permissable.

Plug flow conditions have to be checked. According to Kapteijn and Moulijn [6], the ratio of the inner tube diameter to the particle diameter should be chosen like,

$$\frac{d_i}{d_p} > 10 \tag{10}$$

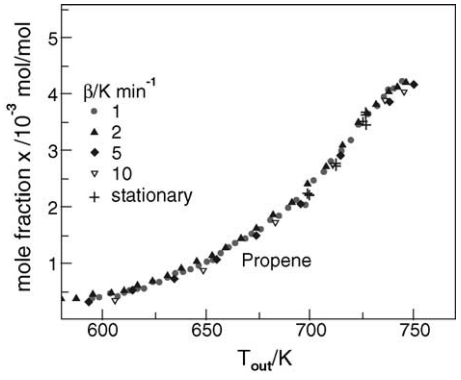

Fig. 2. Mole fractions of propene as a function of temperature for different heating rates.

Table 2
Reynolds numbers in experiments

$\dot{V}_{ref}$ (l_N/min)	T (K)	μ (ms^{-1})	ν (m^2s^{-1})	Re_p
0.5	600	1.48	4.87×10^{-5}	9
	750	1.84	8.05×10^{-5}	7
1.0	600	2.96	4.87×10^{-5}	18
	750	3.70	8.05×10^{-5}	14

Trambouze et al. [7] recommend the following relation for conditions with nearly no axial dispersion:

$$\frac{D_{ax}}{u_{LR}L} < 0.01 \tag{11}$$

These conditions were fulfilled, as the ratio of inner tube diameter to particle diameter was at least 17. The ratio of reactor length and particle diameter was at least 57. The Reynolds number was estimated in the temperature range employed (600–750 K). The thermo-physical data were estimated for nitrogen, which has a mole fraction of 92.5% in the gas. The results are given in Table 2. Plug flow conditions were met.

The radial temperature profile inside the reactor was calculated according to the following expression:

$$T(r) - T_{OVEN} = \frac{2/Bi + 1 - (r/r_i)^2}{2/Bi + 1 - (r^*/r_i)^2}(T^*(r^*) - T_{OVEN}) \tag{12}$$

$$Bi = k_o \frac{r_i}{\lambda_{cat}}; \quad \frac{r^*}{r_i} = 0.6; \quad r_i = 4 \times 10^{-3}\,\text{m} \tag{13}$$

The overall heat transfer coefficient, k_o, is given by 34 W/(m^2 K) (see also Table 1). The Biot number is given by 0.085. The maximum temperature difference between reactor exit and surrounding was measured to be 25 K. Under these conditions, one obtains a temperature difference between the center of the catalyst bed and inner reactor wall of $\Delta T \leq 1$ K. After these preliminary checks, the kinetic measurements were executed. Therefore, there are no distinctive hot spots inside the reactor.

3. Results

The measurements were executed for the conditions as given in Table 3 and some small variations of these values. In Fig. 3, the concentrations and the reaction rates of the reactants are presented. The data evaluation was done as described by Liebner et al. [4]. The reaction rate of the single components was calculated according to:

$$\frac{\dot{n}_{ref}}{\dot{V}_{ref}} \frac{\partial x_i(t_x, \tau_{cat})}{\partial \tau_{cat}}\bigg|_{T_{in}} = \sum \nu_{ak} r_a = r_{TS,k}\,(\text{mol/(kg s)}) \tag{14}$$

The concentrations of reaction products are presented in Fig. 4. One recognises that only about 1.2 mol% of propane were converted, owing to the oxygen limitation. A significant

Table 3
Reactant concentrations corresponding to Figs. 2–4

Reactant concentrations (inlet) (mol%)				Residence time ($kg\,s/m_N^3$)					
				Reference volume flow rate (l_N/min)					
Ne	N_2	C_3H_8	O_2	(□)	(◯)	(△)	(◊)	(▽)	(◁)
5.0	87.50	5.0	2.5	15.0	18.8	21.4	25.0	30.0	37.5
				1.0	0.9	0.8	0.7	0.6	0.5

higher reactants content in the reactant gas mixture leads to such a high exothermicity that the data could not be evaluated in the TSPFR frame. This reveals some limitations of the TSPFR approach for highly exothermic reactions. Because of the total oxidation of propane, oxygen was consumed very fast. For this reason, the rate of reaction of oxygen is four times faster than propane. The products were propene, carbon monoxide, carbon dioxide, water, and traces of ethane, ethene and methane. Propene and carbon monoxide were formed at an amount of 0.5 mol% each. Up to a temperature of 680 K, the rate of reaction is moderate. Between 680 and 700 K, the rate of reaction increases sharply to a maximum at about 730 K and decreases at higher temperatures due to oxygen limitation.

In order to evaluate the measured data, details of the reaction mechanism have to be known. Depending on the catalyst, sometimes a hypothetical reaction mechanism will do. Grabowski et al. [8] concluded by means of transient experiments that the first step of propane conversion follows an Eley–Rideal mechanism. Propane reacts directly from the gas phase with the adsorbed oxygen on the catalyst. Chen et al. [9] showed that propane is dehydrogenated to propene, and in parallel to the total oxidation of propane to carbon dioxide occurs. Carbon monoxide is exclusively created by oxidation of propene. Carbon dioxide is generated by oxidation of propane and propene. Based on these findings, the following reaction scheme was employed:

$$C_3H_8 + 0.5\,O_2 \rightarrow C_3H_6 + H_2O \quad (15)$$

$$C_3H_8 + 5\,O_2 \rightarrow 3\,CO_2 + 4\,H_2O \quad (16)$$

$$C_3H_6 + 3\,O_2 \rightarrow 3\,CO + 3\,H_2O \quad (17)$$

The first equation corresponds to the oxidative dehydrogenation of propane. The second equation assumes that carbon dioxide is primarily formed by oxidation of propane. Oxidation of propene to carbon monoxide is given in the third equation. Some other groups investigated the kinetics of ODH of propane (see, for example, Argyle et al. [10] and Late and Blekken [11], and the literature cited therein). Based on these reactions, three Eley–Rideal-type rate equations were

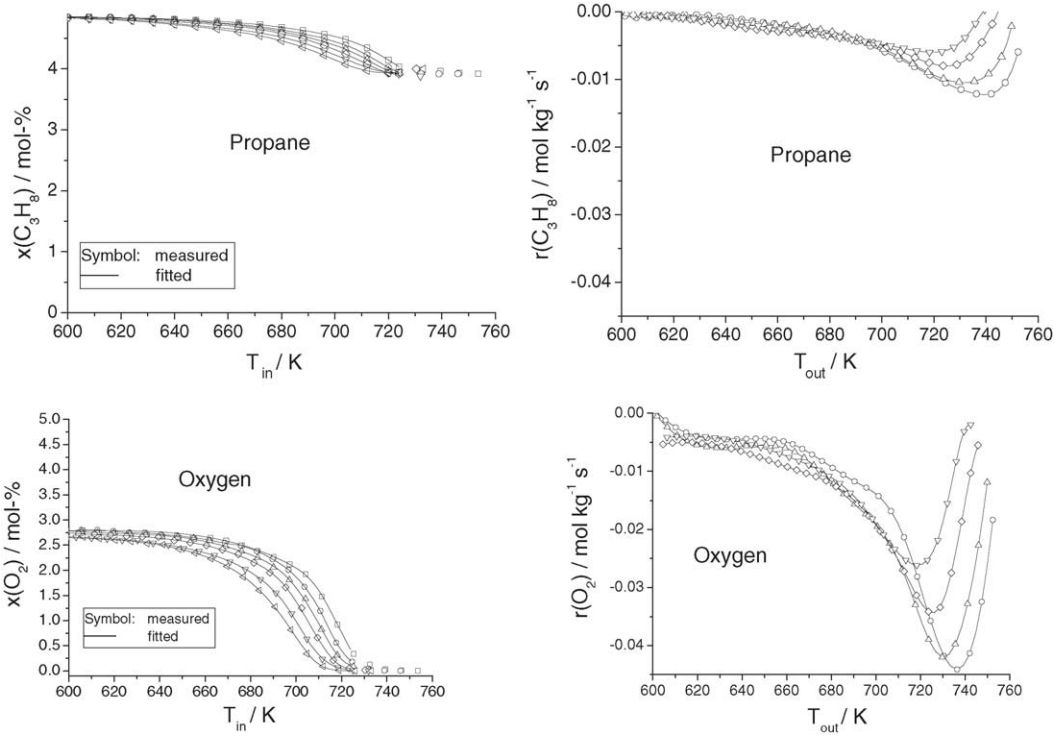

Fig. 3. Reactant concentrations and reaction rates as a function of the inlet and outlet temperature, respectively.

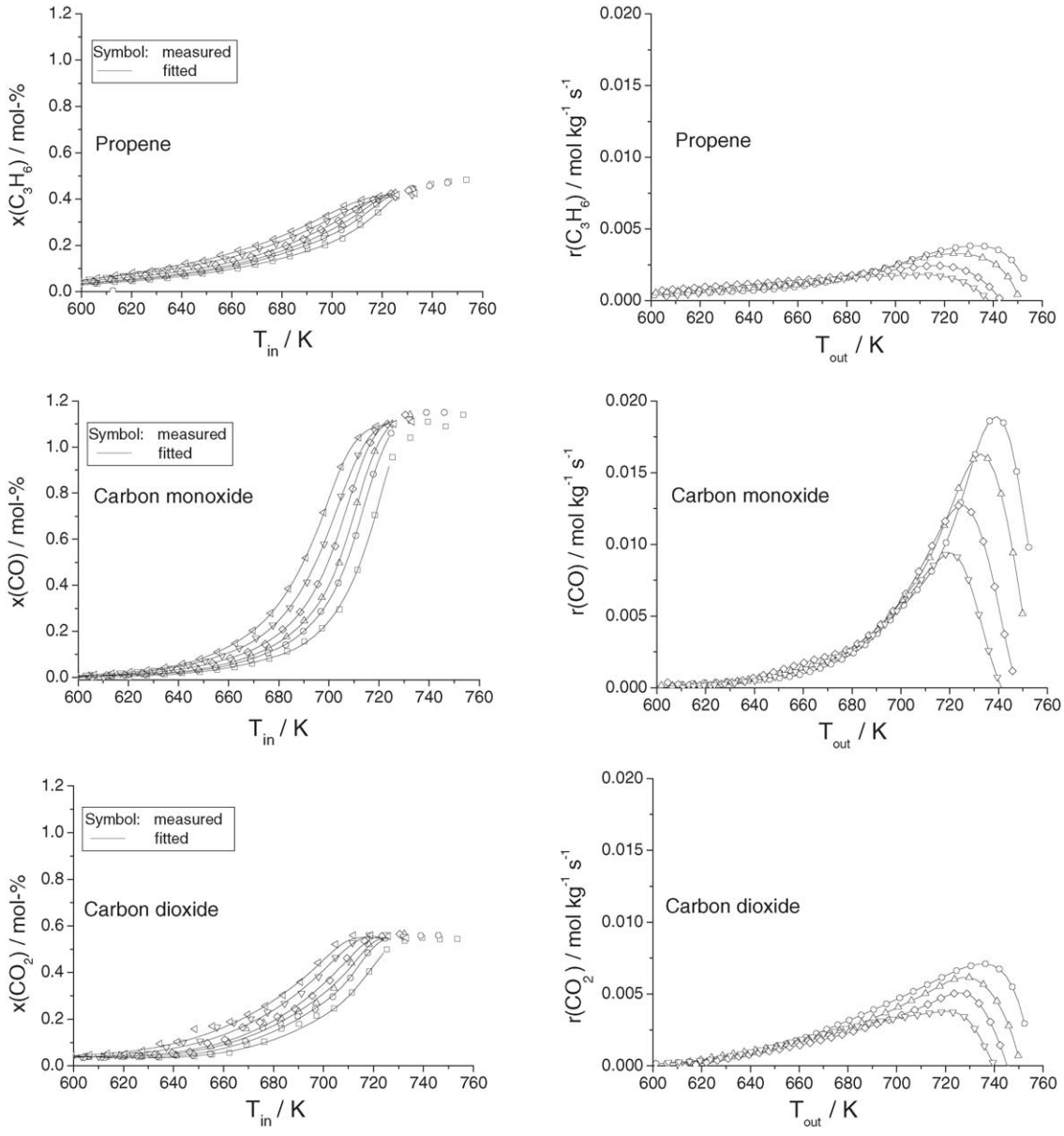

Fig. 4. Product concentration and reaction rates as function of the inlet and outlet temperature, respectively.

introduced:

$$r_{R1} = \frac{k_1 K_{O_2} p_{C_3H_8} p_{O_2}^n}{1 + K_{O_2} p_{O_2}^m} \text{ (mol/(kg s))} \quad (18)$$

$$r_{R2} = \frac{k_2 K_{O_2} p_{C_3H_8} p_{O_2}^n}{1 + K_{O_2} p_{O_2}^m} \text{ (mol/(kg s))} \quad (19)$$

$$r_{R3} = \frac{k_3 K_{O_2} p_{C_3H_6} p_{O_2}^n}{1 + K_{O_2} p_{O_2}^m} \text{ (mol/(kg s))} \quad (20)$$

Amongst the experimental reaction rates, r_{TS}, the following relations exist:

$$r_{TS,r_{R1}} = r_{TS,C_3H_6} + \frac{r_{TS,CO}}{3} \text{ (mol/(kg s))} \quad (21)$$

$$r_{TS,r_{R2}} = \frac{r_{TS,CO_2}}{3} \text{ (mol/(kg s))} \quad (22)$$

$$r_{TS,r_{R2}} = \frac{r_{TS,CO}}{3} \text{ (mol/(kg s))} \quad (23)$$

The parameters of these equations were determined by means of the experimental rates, r_{TS}. The following performance index was minimized by a sequential quadratic programming (SQP) algorithm (NAG library, program E04UCF):

$$Q_r = \sum_{h=1}^{N_j(N_i-2)} (\ln(r_{k,TS,h}) - \ln(r_h))^2 \stackrel{!}{=} \text{MIN} \quad (24)$$

$$r_h = \sum_{a=1}^{N_a} \nu_{ka} r_a \text{ (mol/(kg s))} \quad (25)$$

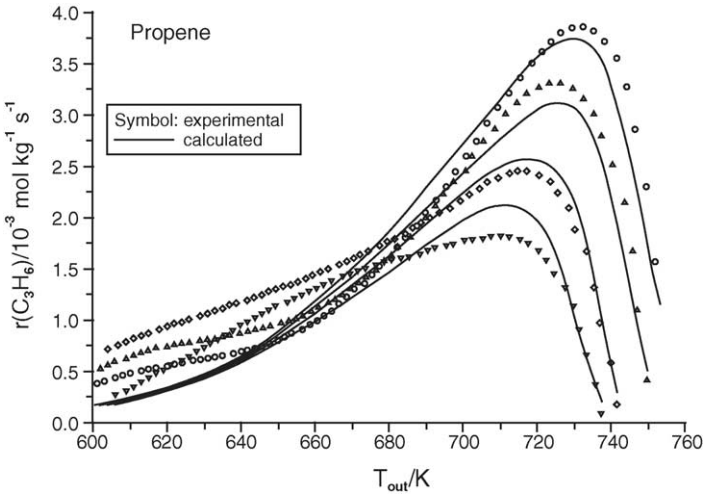

Fig. 5. Reaction rate of propene as a function of temperature.

$$r_a = f(x, T, P, k(t), K(T))\,(\mathrm{mol}/(\mathrm{kg\,s})) \tag{26}$$

$$k(T) = k_\mathrm{o}\,\exp\left(\frac{-E_\mathrm{A}}{RT}\right) \tag{27}$$

The dimension of $k(T)$ depends on the reaction. In our case, it is k mol/(kg Pa s). The results are given in Table 4. Besides Eqs. (18)–(20), Langmuir–Hinshelwood equations were used, but Eqs. (18)–(20) gave the lowest mean square deviation. A Mars-van-Krevelen kinetics was not tested (see, e.g., [11]). The carbon balance showed no coke formation up to 730 K. Above this temperature, some coke formation was obserbed. Argyle et al. [10] found an activation energy for propane ODH and propane combustion of $\sim 115 \pm 20$ kJ/mol and an apparent activation energy for the propene combustion of 60–90 kJ/mol. Similar values were obtained by Late and Blekken [11]. The experimental reaction rates were compared with the calculated rates whereby the fittet parameters were used. The deviations are below ±15%. The fitted data can be employed for a check of the calculated reaction rates of propene. According to Eq. (15), propene is formed from propane, and is oxidized to carbon monoxide (Eq. (17)). The rate of reaction of propene is given by (Eqs. (15)–(17)):

$$r_{\mathrm{C_3H_6}} = r_1 - r_3\,(\mathrm{mol}/(\mathrm{kg\,s})) \tag{28}$$

Table 4
Kinetic parameters of the reactions (Eqs. (18)–(20)) by fitting and optimizing the experimental data

Constant	Parameters	Value
k_1	$k_{1,0}$	6.90 mol/(kg s Pa)
	$E_{\mathrm{A},1}$	104.68 ± 15 kJ/mol
k_2	$k_{2,0}$	5.70 mol/(kg s Pa)
	$E_{\mathrm{A},2}$	83.70 ± 20 kJ/mol
k_3	$k_{3,0}$	8.66 mol/(kg s Pa)
	$E_{\mathrm{A},3}$	79.65 ± 20 kJ/mol
$K_{\mathrm{O_2}}$	$k_{\mathrm{o}2,0} \times 10$	4.02 $\mathrm{Pa}^{-1.5}$
	$E_{\mathrm{A,O_2}}$	49.71 kJ/mol
n, m	–	1.50

The results are given in Fig. 5. The experimental data are identical to the propene data in Fig. 4. In the region between 600 and 660 K, there is a considerable deviation between measurements and calculations. This is the result of imprecision of concentration measurements in this temperature range, as the reaction was not yet ignited. The propene concentration in this temperature range is about 0.2 mol% (compare Fig. 4). Above 680 K, measurements and calculated reaction rates coincide well. This result confirms that the measurements and the reaction rates calculated from them are consistent. Likelihood regions of kinetic parameters were also calculated. For this purpose, the kinetic parameters occurring in the reaction rate equations were pair wise varied, and the deviations from the minimum of the performance index (see Eq. (24)) were plotted at 10, 20 and 30%. There are five possible combinations for each of the three reactions (see Eqs. (15)–(17)). It was found that the deviations are largest for cases where the parameters are coupled as products of the Arrhenius equation. This holds for $k_{1,2,3}$ and $K_{\mathrm{O_2}}$.

Not in the present example, but in principle a very high exothermicity of reactions may lead to difficulties within the TSPFR scheme because of too large radial temperature profiles. For such a case, one could redesign the reactor. Two coaxial cylinders could be used where the inner cylinder and the annulus are filled with the same catalyst. By employing a proper volumetric flow rate of the reactants in the inner tube and the annulus, nearly the same temperature profiles are created inside the inner tube and the annulus, which minimizes the uneven heat flow from the inner tube to the surrounding gas in the oven. Whether this modification is sufficient, has to be checked. Parallel reactors can further accelerate the TSPFR measurements.

4. Conclusion

In the present investigation, the concept of the TSPFR was employed to a complex reaction system. Like the case of ammonia formation from hydrogen and nitrogen, the kinetics of oxidative dehydrogenation of propane could be described satisfactorily by the TSPFR approach, provided that the propane content in the reactant mixture was kept below a certain value. For extremely exothermic reactions, the TSPFR approach cannot be employed without modifications. Nevertheless, in general a large amount of data can be obtained in a rather short time, leading to a well-founded basis of kinetic modelling.

References

[1] B.W. Wojchiekowski, The temperature-scanning reactor I: reactor types and modes of operation, Catal. Today 36 (1997) 167–190.
[2] N.M. Rice, B.W. Wojciechowski, The temperature-scanning reactor II: theory of operation, Catal. Today 36 (1997) 191–207.
[3] S.P. Asprey, N.M. Rice, B.W. Wojciechowski, The temperature-scanning reactor III: experimental procedures and data processing, Catal. Today 36 (1997) 209–226.
[4] C. Liebner, D. Wolf, M. Baerns, M. Kolkowski, F.J. Keil, A high-speed method for obtaining kinetic data for exothermic and endothermic catalytic reactions under non-isothermal conditions illustrated for the ammonia synthesis, Appl. Catal. A 240 (2003) 95–110.
[5] M. Kolkowski, J. Malachowski, F.J. Keil, C. Liebner, D. Wolf, M. Baerns, Influences of heat transport on the determination of reaction rates using the temperature-scanning plug flow reactor, Chem. Eng. Sci. 58 (2003) 4903–4909.
[6] F. Kapteijn, J.A. Moulijn, in: G. Ertl, H. Knözinger, J. Weitkamp (Eds.), Handbook of Heterogeneous Catalysis, vol. 3, VCH, Weinheim, 1997, pp. 1359–1376.
[7] P. Trambouze, H. van Landeghem, J.-P. Wauquier, Chemical Reactors, Gulf Publishing Co., Houston, 1988.
[8] R. Grabowski, S. Pietrzyk, J. Soczynski, F. Genser, K. Wcisco, B. Grzybowska-Swierkosz, Kinetics of propane oxidative dehydrogenation on vanadia/titania catalysts from steady state and transient experiments, Appl. Catal. A 232 (2002) 277–288.
[9] K. Chen, A. Khadakov, J. Yang, A.T. Bell, E. Iglesia, Isotopic tracer and kinetic studies of oxidative dehydrogenation pathways on vanadium oxide catalysts, J. Catal. 186 (1999) 325–333.
[10] M.D. Argyle, K. Chen, A.T. Bell, E. Iglesia, Effect of catalyst structure on oxidative dehydrogenation of ethane and propene on alumina-supported vanadia, J. Catal. 208 (2002) 139–149.
[11] L. Late, E.A. Blekken, Kinetics of the oxidative dehydrogenation of propane over VMgO catalyst, J. Nat. Gas Chem. 11 (2002) 33–42.